NASA TN D-3999

EFFECTS OF COMBINED BUOYANCY AND SHEAR ON WEAK HOMOGENEOUS TURBULENCE

By Robert G. Deissler

Lewis Research Center
Cleveland, Ohio

NATIONAL AERONAUTICS AND SPACE ADMINISTRATION

For sale by the Clearinghouse for Federal Scientific and Technical Information
Springfield, Virginia 22151 - CFSTI price $3.00

EFFECTS OF COMBINED BUOYANCY AND SHEAR ON WEAK HOMOGENEOUS TURBULENCE

by Robert G. Deissler

Lewis Research Center

SUMMARY

A simplified model is analyzed in order to give some insight into the effects of buoyancy and shear flow on turbulence. Two-point correlation equations, which contain mean velocity and temperature gradients, as well as body force terms, can be constructed from the Navier-Stokes, energy, and continuity equations. While previous papers by the author considered the effects of shear and buoyancy separately, the present paper considers their combined effects. In that case the ratio of buoyancy to shear effects, as given by the Richardson number, is a consideration. The velocity and temperature gradients, as well as the body force, are considered to be vertical and uniform.

An initial value problem in which the turbulence is initially isotropic is solved to illustrate the effect of buoyancy and shear parameters on the turbulence. The initially isotropic turbulence quickly becomes anisotropic under the influence of the buoyancy and shear. Although the turbulence is assumed to be weak enough for terms in the equations containing triple correlations to be negligible, a term proportional to the velocity gradient transfers energy between wave numbers. Various components of the mean turbulent fluctuations and their spectra, as well as the ratio of eddy conductivity to eddy viscosity, are calculated as functions of buoyance and shear parameters. For highly stabilizing conditions, the interaction of the shear and buoyancy forces with the turbulence can produce negative eddy conductivities and viscosities. The analytical results are compared with available experimental data.

INTRODUCTION

The effects of buoyancy and of shear on weak homogeneous turbulence are considered separately in reference 1 and 2. In real situations, for instance in the atomsphere, the

two effects often occur simultaneously. The speculative theories given in references 3 and 4 consider that case.

In the present paper, the methods used in references 1 and 2 are extended to analyze the combined effects of buoyancy and shear on homogeneous turbulence. Correlation equations for velocities and temperatures at two points in the turbulent field are constructed from the Navier-Stokes, energy, and continuity equations. In order to obtain a determinate set of equations, the turbulence is assumed to be weak enough to neglect the terms in the equations containing triple correlations. Although this assumption may limit the upper Reynolds number for which the analysis is valid, the analysis is of interest in itself, in that it gives an asymptotically exact solution for turbulence in the limit of low Reynolds numbers. Moreover, when mean velocity and temperature gradient terms are present in the equations, the turbulence may not have to be as weak as it would otherwise for the triple correlation terms to be negligible compared with the other terms. As will be seen later, comparison of the analysis with experiment indicates that the theoretical results bear a correspondence with real turbulence at moderate Reynolds numbers.

The correlation and spectral equations required in the analysis will be considered in the next section.

BASIC EQUATIONS

The Navier-Stokes equation with buoyancy effects included can be written as (ref. 5)

$$\frac{\partial \tilde{u}_i}{\partial t} + \frac{\partial(\tilde{u}_i \tilde{u}_k)}{\partial x_k} = -\frac{1}{\rho}\frac{\partial}{\partial x_i}(p - p_e) + \nu \frac{\partial^2 \tilde{u}_i}{\partial x_k \, \partial x_k} - \beta(\tilde{T} - T_e)g_i \tag{1}$$

where the subscripts (except e) can take on the values 1, 2, or 3, and a repeated subscript in a term signifies a summation. The quantity $\tilde{u}_i$ is an instantaneous velocity component, $\tilde{T}$ is the instantaneous temperature, x_i is a space coordinate, t is the time, ρ is the density, ν is the kinematic viscosity, p is the instantaneous pressure, g_i is a component of the body force, and $\beta \equiv -(1/\rho)(\partial\rho/\partial T)_p$ is the thermal expansion coefficient of the fluid. The quantities T_e and p_e are the equilibrium temperature and pressure, respectively. (All symbols are given in the appendix.) In obtaining the last term in equation (1) (buoyancy term), the density is assumed to depend effectively only on temperature and is not far removed from its equilibrium value (value it would have for no heat transfer). Note that the equilibrium temperature is uniform whereas the equilibrium pressure is not. The instantaneous velocities and temperatures in equation (1) can be divided into mean and fluctuating components as follows:

$$\tilde{u}_i = U_i + u_i \tag{2}$$

$$\tilde{T} = T + \tau \tag{3}$$

Then, if equation (1) is averaged, and the averaged equation is subtracted from the unaveraged one,

$$\frac{\partial u_i}{\partial t} + u_k \frac{\partial U_i}{\partial x_k} + U_k \frac{\partial u_i}{\partial x_k} + \frac{\partial (u_i u_k)}{\partial x_k} - \frac{\partial \overline{u_i u_k}}{\partial x_k} = -\frac{1}{\rho} \frac{\partial (p - p_e)}{\partial x_i} + \nu \frac{\partial^2 u_i}{\partial x_k \partial x_k} - \beta g_i \tau \tag{4}$$

Taking the divergence of equation (4) (differentiating with respect to x_i) and using continuity give

$$\frac{1}{\rho} \frac{\partial^2 (p - p_e)}{\partial x_i \partial x_i} = -2 \frac{\partial u_i}{\partial x_k} \frac{\partial U_k}{\partial x_i} - \frac{\partial^2 (u_i u_k)}{\partial x_i \partial x_k} + \frac{\partial^2 \overline{u_i u_k}}{\partial x_i \partial x_k} - \beta g_i \frac{\partial \tau}{\partial x_i} \tag{5}$$

The instantaneous energy equation can be written as

$$\frac{\partial \tilde{T}}{\partial t} + \frac{\partial (\tilde{T} \tilde{u}_k)}{\partial x_k} = \alpha \frac{\partial^2 \tilde{T}}{\partial x_k \partial x_k} \tag{6}$$

Substituting equations (2) and (3) in equation (6), averaging, and subtracting the averaged equation from the unaveraged one give

$$\frac{\partial \tau}{\partial t} + u_k \frac{\partial T}{\partial x_k} + U_k \frac{\partial \tau}{\partial x_k} + \frac{\partial (\tau u_k)}{\partial x_k} - \frac{\partial \overline{\tau u_k}}{\partial x_k} = \alpha \frac{\partial^2 \tau}{\partial x_k \partial x_k} \tag{7}$$

Equations (4), (5), and (7) apply at a point P in the turbulent fluid. Similar equations at another point P' can be obtained simply by priming the variables and changing the subscript i to, say, j. Equations involving correlations between fluctuating quantities at P and P' can then be constructed by methods similar to those used in references 1, 2, and 6. In fact, the equations considered in those references are special cases of those obtained here. The resulting equations for homogeneous turbulence with uniform velocity and temperature gradients are

$$\frac{\partial \overline{u_i u_j'}}{\partial t} + \overline{u_k u_j'} \frac{\partial U_i}{\partial x_k} + \overline{u_i u_k'} \frac{\partial U_j}{\partial x_k} + (U_k' - U_k) \frac{\partial \overline{u_i u_j'}}{\partial r_k} + \frac{\partial}{\partial r_k} \left(\overline{u_i u_j' u_k'} - \overline{u_i u_k u_j'} \right)$$

$$= -\frac{1}{\rho} \left(\frac{\partial \overline{u_i p'}}{\partial r_j} - \frac{\partial \overline{p u_j'}}{\partial r_i} \right) + 2\nu \frac{\partial^2 \overline{u_i u_j'}}{\partial r_k \, \partial r_k} - \beta g_i \overline{\tau u_j'} - \beta g_j \overline{u_i \tau'} \qquad (8)$$

$$\frac{\partial \overline{\tau \tau'}}{\partial t} + \overline{u_k \tau'} \frac{\partial T}{\partial x_k} + \overline{\tau u_k'} \frac{\partial T}{\partial x_k} + (U_k' - U_k) \frac{\partial \overline{\tau \tau'}}{\partial r_k} + \frac{\partial}{\partial r_k} \left(\overline{\tau \tau' u_k'} - \overline{\tau u_k \tau'} \right) = 2\alpha \frac{\partial^2 \overline{\tau \tau'}}{\partial r_k \, \partial r_k} \qquad (9)$$

$$\frac{\partial \overline{\tau u_j'}}{\partial t} + \overline{u_k u_j'} \frac{\partial T}{\partial x_k} + \overline{\tau u_k'} \frac{\partial U_j}{\partial x_k} + (U_k' - U_k) \frac{\partial \overline{\tau u_j'}}{\partial r_k} + \frac{\partial}{\partial r_k} \left(\overline{\tau u_j' u_k'} - \overline{\tau u_k u_j'} \right)$$

$$= -\frac{1}{\rho} \frac{\partial \overline{\tau p'}}{\partial r_j} + (\alpha + \nu) \frac{\partial^2 \overline{\tau u_j'}}{\partial r_k \, \partial r_k} - \beta g_j \overline{\tau \tau'} \qquad (10)$$

$$\frac{\partial \overline{u_i \tau'}}{\partial t} + \overline{u_i u_k'} \frac{\partial T}{\partial x_k} + \overline{u_k \tau'} \frac{\partial U_i}{\partial x_k} + (U_k' - U_k) \frac{\partial \overline{u_i \tau'}}{\partial r_k} + \frac{\partial}{\partial r_k} \left(\overline{u_i \tau' u_k'} - \overline{u_i u_k \tau'} \right)$$

$$= \frac{1}{\rho} \frac{\overline{\partial p \tau'}}{\partial r_i} + (\alpha + \nu) \frac{\partial^2 \overline{u_i \tau'}}{\partial r_k \, \partial r_k} - \beta g_i \overline{\tau \tau'} \qquad (11)$$

$$\frac{1}{\rho} \frac{\partial^2 \overline{u_i p'}}{\partial r_j \, \partial r_j} = -2 \frac{\partial \overline{u_i u_k'}}{\partial r_j} \frac{\partial U_j}{\partial x_k} - \frac{\partial^2 \overline{u_i u_j' u_k'}}{\partial r_j \, \partial r_k} - \beta g_j \frac{\partial \overline{u_i \tau'}}{\partial r_j} \qquad (12)$$

$$\frac{1}{\rho} \frac{\partial^2 \overline{p u_j'}}{\partial r_i \, \partial r_i} = 2 \frac{\partial \overline{u_i u_j'}}{\partial r_k} \frac{\partial U_k}{\partial x_i} - \frac{\partial^2 \overline{u_i u_k u_j'}}{\partial r_i \, \partial r_k} + \beta g_i \frac{\partial \overline{\tau u_j'}}{\partial r_i} \qquad (13)$$

$$\frac{1}{\rho} \frac{\partial^2 \overline{p \tau'}}{\partial r_i \, \partial r_i} = 2 \frac{\partial \overline{u_i \tau'}}{\partial r_k} \frac{\partial U_k}{\partial x_i} - \frac{\partial^2 \overline{u_i u_k \tau'}}{\partial r_i \, \partial r_k} + \beta g_i \frac{\partial \overline{\tau \tau'}}{\partial r_i} \qquad (14)$$

$$\frac{1}{\rho}\frac{\partial^2\overline{\tau p'}}{\partial r_j\,\partial r_j} = -2\frac{\partial\overline{\tau u_k'}}{\partial r_j}\frac{\partial U_j}{\partial x_k} - \frac{\partial^2\overline{\tau u_j' u_k'}}{\partial r_j\,\partial r_k} - \beta g_j\frac{\partial\overline{\tau\tau'}}{\partial r_j} \tag{15}$$

Equations (8) to (15) form a determinate set if the turbulence is weak enough to neglect terms containing triple correlations in comparison with the other terms. They can be converted to spectral form by introducing three-dimensional Fourier transforms defined as follows:

$$\overline{u_i u_j'} = \int_{-\infty}^{\infty} \varphi_{ij} e^{i\vec{\kappa}\cdot\vec{r}}\, d\vec{\kappa} \tag{16}$$

$$\overline{pu_j'} = \int_{-\infty}^{\infty} \lambda_j e^{i\vec{\kappa}\cdot\vec{r}}\, d\vec{\kappa} \tag{17}$$

$$\overline{u_i p'} = \int_{-\infty}^{\infty} \lambda_i' e^{i\vec{\kappa}\cdot\vec{r}}\, d\vec{\kappa} \tag{18}$$

$$\overline{p\tau'} = \int_{-\infty}^{\infty} \zeta e^{i\vec{\kappa}\cdot\vec{r}}\, d\vec{\kappa} \tag{19}$$

$$\overline{\tau p'} = \int_{-\infty}^{\infty} \zeta' e^{i\vec{\kappa}\cdot\vec{r}}\, d\vec{\kappa} \tag{20}$$

$$\overline{\tau u_j'} = \int_{-\infty}^{\infty} \gamma_j e^{i\vec{\kappa}\cdot\vec{r}}\, d\vec{\kappa} \tag{21}$$

$$\overline{u_i\tau'} = \int_{-\infty}^{\infty} \gamma_i' e^{i\vec{\kappa}\cdot\vec{r}}\, d\vec{\kappa} \tag{22}$$

$$\overline{\tau\tau'} = \int_{-\infty}^{\infty} \delta e^{i\vec{\kappa}\cdot\vec{r}}\, d\vec{\kappa} \tag{23}$$

where $\vec{\kappa}$ is the wave number vector and $d\vec{\kappa} = d\kappa_1\, d\kappa_2\, d\kappa_3$. The magnitude of $\vec{\kappa}$ has the dimension 1/length and can be considered to be the reciprocal of a wavelength or eddy size. Then, from equation (16) (see eq. (10), ref. 7),

$$r_3 \frac{\partial \overline{u_i u_j'}}{\partial r_1} = - \int_{-\infty}^{\infty} \kappa_1 \frac{\partial \varphi_{ij}}{\partial \kappa_3} e^{i\vec{\kappa} \cdot \vec{r}} \, d\vec{\kappa} \tag{24}$$

The remainder of the paper will present the case where the velocity and the temperature gradients are in the x_3-direction (vertical) and the body force (gravity) is in the $-x_3$-direction. Then, let

$$g \equiv -g_3 \tag{25}$$

$$a = \frac{dU_1}{dx_3} \tag{26}$$

$$b = \frac{dT}{dx_3} \tag{27}$$

and neglect terms containing triple correlations; equations (8) to (15) become, in spectral form,

$$\frac{\partial \varphi_{ij}}{\partial t} + \delta_{i1} a \varphi_{3j} + \delta_{j1} a \varphi_{i3} - a\kappa_1 \frac{\partial \varphi_{ij}}{\partial \kappa_3} = -\frac{1}{\rho} (i\kappa_j \lambda_i' - i\kappa_i \lambda_j) - 2\nu\kappa^2 \varphi_{ij} + \beta\delta_{i3} g\gamma_j + \beta\delta_{j3} g\gamma_i' \tag{28}$$

$$\frac{\partial \delta}{\partial t} + b\gamma_3' + b\gamma_3 - a\kappa_1 \frac{\partial \delta}{\partial \kappa_3} = -2\alpha\kappa^2 \delta \tag{29}$$

$$\frac{\partial \gamma_j}{\partial t} + b\varphi_{3j} + a\delta_{1j}\gamma_3 - a\kappa_1 \frac{\partial \gamma_j}{\partial \kappa_3} = -\frac{1}{\rho} i\kappa_j \zeta' - (\alpha + \nu)\kappa^2 \gamma_j + \beta g \delta_{j3} \delta \tag{30}$$

$$\frac{\partial \gamma_i'}{\partial t} + b\varphi_{i3} + a\delta_{i1}\gamma_3' - a\kappa_1 \frac{\partial \gamma_i'}{\partial \kappa_3} = -(\alpha + \nu)\kappa^2 \gamma_i' + \frac{1}{\rho} i\kappa_i \zeta + \beta g \delta_{i3} \delta \tag{31}$$

$$-\frac{1}{\rho} \kappa^2 \lambda_i' = -2ai\kappa_1 \varphi_{i3} + \beta g i \kappa_3 \gamma_i' \tag{32}$$

$$-\frac{1}{\rho}\kappa^2\lambda_j = 2ai\kappa_1\varphi_{3j} - \beta gi\kappa_3\gamma_j \tag{33}$$

$$-\frac{1}{\rho}\kappa^2\zeta = 2ai\kappa_1\gamma_3' - \beta gi\kappa_3\delta \tag{34}$$

$$-\frac{1}{\rho}\kappa^2\zeta' = -2ai\kappa_1\gamma_3 + \beta gi\kappa_3\delta \tag{35}$$

where δ_{ij} is the Kronecker delta. Substitution of equations (32) to (35) into equations (28) to (31) shows that $\varphi_{ij} = \varphi_{ji}$ and $\gamma_i = \gamma_i'$ for all times if they are equal at an initial time. It will be assumed herein that the turbulence is initially isotropic and that the temperature fluctuations are initially zero, so that the above relations will hold. Thus, the set of equations (28) to (35) becomes

$$\frac{\partial\varphi_{ij}}{\partial t} = a\kappa_1\frac{\partial\varphi_{ij}}{\partial\kappa_3} - a(\delta_{i1}\varphi_{j3} + \delta_{1j}\varphi_{i3}) + 2a\left(\frac{\kappa_1\kappa_j}{\kappa^2}\varphi_{i3} + \frac{\kappa_i\kappa_1}{\kappa^2}\varphi_{j3}\right)$$

$$+ \beta g\gamma_i\left(\delta_{j3} - \frac{\kappa_3\kappa_j}{\kappa^2}\right) + \beta g\gamma_j\left(\delta_{i3} - \frac{\kappa_i\kappa_3}{\kappa^2}\right) - 2\nu\kappa^2\varphi_{ij} \tag{36}$$

$$\frac{\partial\gamma_i}{\partial t} = a\kappa_1\frac{\partial\gamma_i}{\partial\kappa_3} - b\varphi_{i3} + a\gamma_3\left(2\frac{\kappa_i\kappa_1}{\kappa^2} - \delta_{i1}\right) + \beta g\delta\left(\delta_{i3} - \frac{\kappa_i\kappa_3}{\kappa^2}\right) - (\alpha + \nu)\kappa^2\gamma_i \tag{37}$$

$$\frac{\partial\delta}{\partial t} = a\kappa_1\frac{\partial\delta}{\partial\kappa_3} - 2b\gamma_3 - 2\alpha\kappa^2\delta \tag{38}$$

Equations (36), (37), and (38) give contributions of various processes to the rates of change of spectral components of $\overline{u_iu_j}$, $\overline{\tau u_i}$, and $\overline{\tau^2}$, respectively. The second term in each equation is a transfer term which transfers activity into or out of a spectral component by the stretching or compressing of turbulent vortex filaments by the mean velocity gradient, as discussed in references 2, 6, and 7. The terms with κ^2 in the denominator are spectral components of pressure-velocity or pressure-temperature correlations and transfer activity between directional components (ref. 2). The terms proportional to βg and δ_{i3} (or δ_{j3}) are buoyancy terms which augment or diminish the activity in a spectral component by buoyant action. The last terms in the equations are dissipation terms, which dissipate activity by viscous effects (eq. (36)) or by conduction effects

(eq. (38)). The dissipation term in equation (37) contains both viscous and conduction effects, inasmuch as it dissipates spectral components of velocity-temperature correlations. The remaining terms in the equations produce activity by velocity or temperature gradient effects. Although a buoyancy term does not appear in equation (38), buoyancy affects δ (or $\overline{\tau^2}$) indirectly through the temperature gradient and γ_3 (or $\overline{\tau u_3}$).

For solving equations (36) to (38), the turbulence is assumed to be initially isotropic at $t = t_0$. That condition is satisfied by the relation

$$(\varphi_{ij})_0 = \frac{J_0}{12\pi^2}(\kappa^2\delta_{ij} - \kappa_i\kappa_j) \tag{39}$$

where J_0 is a constant that depends on initial conditions (ref. 2, eq. (43)). For the initial conditions of δ and γ_i (at $t = t_0$), it is assumed that

$$\delta_0 = (\gamma_i)_0 = 0 \tag{40}$$

That is, the turbulence-producing grid is assumed to be unheated, so that the temperature fluctuations are produced by the interactions of the mean temperature gradient with the turbulence.

SOLUTION OF SPECTRAL EQUATIONS

In order to reduce the set of partial differential equations, equations (36) to (38), to ordinary differential equations, the running variables ξ and η are considered, of which κ_3 and t are particular values such that $\xi = \kappa_3$ when $\eta = t$. If ξ and η are introduced into the set of equations in place of κ_3 and t, the resulting equations will, of course, automatically satisfy the original set. In addition,

$$\xi + a\kappa_1(\eta - \eta_0) = \text{constant} \tag{41}$$

during integration. Then

$$\left(\frac{\partial}{\partial\xi}\right)_\eta - \frac{1}{a\kappa_1}\left(\frac{\partial}{\partial\eta}\right)_\xi = \left(\frac{d}{d\xi}\right)_{\xi + a\kappa_1\eta} \tag{42}$$

where the subscripts outside the parentheses signify quantities which are held constant.

Then equations (36) to (38) become

$$\frac{d\varphi_{33}(\xi)}{d\xi} = -4\frac{\xi\varphi_{33}}{\kappa_1^2+\kappa_2^2+\xi^2} - 2\frac{\beta g}{a\kappa_1}\left(1-\frac{\xi^2}{\kappa_1^2+\kappa_2^2+\xi^2}\right)\gamma_3 + 2\nu\frac{\kappa_1^2+\kappa_2^2+\xi^2}{a\kappa_1}\varphi_{33} \tag{43}$$

$$\frac{d\gamma_3(\xi)}{d\xi} = \frac{b}{a\kappa_1}\varphi_{33} - 2\frac{\xi\gamma_3}{\kappa_1^2+\kappa_2^2+\xi^2} - \frac{\beta g}{a\kappa_1}\left(1-\frac{\xi^2}{\kappa_1^2+\kappa_2^2+\xi^2}\right)\delta + \left(\frac{\alpha}{\nu}+1\right)\nu\frac{\kappa_1^2+\kappa_2^2+\xi^2}{a\kappa_1}\gamma_3 \tag{44}$$

$$\frac{d\delta(\xi)}{d\xi} = \frac{2b}{a\kappa_1}\gamma_3 + 2\alpha\frac{\kappa_1^2+\kappa_2^2+\xi^2}{a\kappa_1}\delta \tag{45}$$

$$\frac{d\varphi_{13}(\xi)}{d\xi} = \frac{\varphi_{33}}{\kappa_1} - 2\frac{(\xi\varphi_{13}+\kappa_1\varphi_{33})}{\kappa_1^2+\kappa_2^2+\xi^2} - \frac{\beta g}{a\kappa_1}\left(1-\frac{\xi^2}{\kappa_1^2+\kappa_2^2+\xi^2}\right)\gamma_1$$

$$+\frac{\beta g}{a}\frac{\xi\gamma_3}{\kappa_1^2+\kappa_2^2+\xi^2} + 2\nu\frac{\kappa_1^2+\kappa_2^2+\xi^2}{a\kappa_1}\varphi_{13} \tag{46}$$

$$\frac{d\varphi_{11}(\xi)}{d\xi} = \frac{2}{\kappa_1}\varphi_{13} - 4\frac{\kappa_1\varphi_{13}}{\kappa_1^2+\kappa_2^2+\xi^2} + \frac{2\beta g\xi\gamma_1}{a(\kappa_1^2+\kappa_2^2+\xi^2)} + 2\nu\frac{\kappa_1^2+\kappa_2^2+\xi^2}{a\kappa_1}\varphi_{11} \tag{47}$$

$$\frac{d\varphi_{ii}(\xi)}{d\xi} = \frac{2}{\kappa_1}\varphi_{13} - \frac{2\beta g\gamma_3}{a\kappa_1} + 2\nu\frac{\kappa_1^2+\kappa_2^2+\xi^2}{a\kappa_1}\varphi_{ii} \tag{48}$$

$$\frac{d\gamma_1(\xi)}{d\xi} = \frac{b\varphi_{13}}{a\kappa_1} - \left(2\frac{\kappa_1}{\kappa_1^2+\kappa_2^2+\xi^2} - \frac{1}{\kappa_1}\right)\gamma_3 + \frac{\beta g\xi\delta}{a(\kappa_1^2+\kappa_2^2+\xi^2)} + \left(\frac{\alpha}{\nu}+1\right)\nu\frac{\kappa_1^2+\kappa_2^2+\xi^2}{a\kappa_1}\gamma_1 \tag{49}$$

Note that the first three of these equations are independent of the remaining ones.

The constant in equation (41) subject to the initial conditions, equations (39) and (40), may be determined by letting $\xi = \xi_0$ when $\eta = \eta_0$, or $\xi_0 = \xi + a\kappa_1(\eta - \eta_0)$. This equation applies for any value of ξ, and thus

$$\xi_0 = \kappa_3 + a\kappa_1(t - t_0) \tag{50}$$

Equation (50) gives the value of ξ at which to start the integration for given values of κ_3, κ_1, a, and $t - t_0$. The initial conditions, equations (39) and (40), may be satisfied by letting

$$\left.\begin{aligned}
\varphi_{33}(\xi) &= \frac{J_0}{12\pi^2}\left(\kappa_1^2 + \kappa_2^2\right) \\
\varphi_{13}(\xi) &= -\frac{J_0}{12\pi^2}\kappa_1\xi_0 \\
\varphi_{11}(\xi) &= \frac{J_0}{12\pi^2}\left(\kappa_2^2 + \xi_0^2\right) \\
\varphi_{ii} &= \frac{J_0}{6\pi^2}\left(\kappa_1^2 + \kappa_2^2 + \xi_0^2\right) \\
\gamma_i(\xi) &= \delta(\xi) = 0
\end{aligned}\right\} \text{when } \xi = \xi_0$$

The integration of equation (43) to (49) then goes from ξ_0 to $\xi = \kappa_3$. Final values of φ_{ij}, γ_i, and δ, for which $\xi = \kappa_3$ and $\eta = t$ are of interest. The quantity ξ can be considered as a dummy variable of integration.

The following dimensionless quantities are introduced in order to convert equations (43) to (49) to dimensionless form:

$$\kappa_i^* = \nu^{1/2}(t - t_0)^{1/2}\,\kappa_i \tag{51}$$

$$\xi^* = \nu^{1/2}(t - t_0)^{1/2}\,\xi \tag{52}$$

$$\varphi_{ij}^* = \frac{\nu(t - t_0)}{J_0}\varphi_{ij} \tag{53}$$

$$\gamma_i^* = \frac{\nu}{J_0 b}\gamma_i \tag{54}$$

$$\delta^* = \frac{\nu\delta}{J_0 b^2 (t - t_0)} \tag{55}$$

$$a^* = (t - t_0)a \tag{56}$$

$$Ri = \frac{\beta g b}{a^2} \tag{57}$$

$$Pr = \frac{\nu}{\alpha} \tag{58}$$

In addition, spherical coordinates are introduced into the equations by using the transformations

$$\left.\begin{aligned} \kappa_1 &= \kappa \cos\varphi \sin\theta \\ \kappa_2 &= \kappa \sin\varphi \sin\theta \\ \kappa_3 &= \kappa \cos\theta \end{aligned}\right\} \tag{59}$$

Equations (43) to (49) then become

$$\frac{d\varphi_{33}^*(\xi^*)}{d\xi^*} = -4 \frac{\xi^* \varphi_{33}^*}{\kappa^{*2} \sin^2\theta + \xi^{*2}} - 2 \frac{a^* Ri}{\kappa^* \cos\varphi \sin\theta} \left(1 - \frac{\xi^{*2}}{\kappa^{*2} \sin^2\theta + \xi^{*2}}\right) \gamma_3^*$$

$$+ 2 \frac{\kappa^{*2} \sin^2\theta + \xi^{*2}}{a^* \kappa^* \cos\varphi \sin\theta} \varphi_{33}^* \tag{60}$$

$$\frac{d\gamma_3^*(\xi^*)}{d\xi^*} = \frac{\varphi_{33}^*}{a^* \kappa^* \cos\varphi \sin\theta} - \frac{2\xi^* \gamma_3^*}{\kappa^{*2} \sin^2\theta + \xi^{*2}} - \frac{a^* Ri \delta^*}{\kappa^* \cos\varphi \sin\theta} \left(1 - \frac{\xi^{*2}}{\kappa^{*2} \sin^2\theta + \xi^{*2}}\right)$$

$$+ \left(\frac{1}{Pr} + 1\right) \frac{\kappa^{*2} \sin^2\theta + \xi^{*2}}{a^* \kappa^* \cos\varphi \sin\theta} \gamma_3^* \tag{61}$$

$$\frac{d\delta^*(\xi^*)}{d\xi^*} = \frac{2\gamma_3^*}{a^*\kappa^* \cos\varphi \sin\theta} + \frac{2}{Pr} \frac{\kappa^{*2} \sin^2\theta + \xi^{*2}}{a^*\kappa^* \cos\varphi \sin\theta} \delta^* \tag{62}$$

$$\frac{d\varphi_{13}^*(\xi^*)}{d\xi^*} = \frac{\varphi_{33}^*}{\kappa^* \cos\varphi \sin\theta} - 2 \frac{(\xi^*\varphi_{13}^* + \kappa^* \cos\varphi \sin\theta \varphi_{33}^*)}{\kappa^{*2} \sin^2\theta + \xi^{*2}}$$

$$- \frac{a^*Ri\gamma_1^*}{\kappa^* \cos\varphi \sin\theta} \left(1 - \frac{\xi^{*2}}{\kappa^{*2} \sin^2\theta + \xi^{*2}}\right) + \frac{a^*Ri\xi^*\gamma_3^*}{\kappa^{*2} \sin^2\theta + \xi^{*2}} + 2 \frac{\kappa^{*2} \sin^2\theta + \xi^{*2}}{a^*\kappa^* \cos\varphi \sin\theta} \varphi_{13}^* \tag{63}$$

$$\frac{d\varphi_{ii}^*(\xi^*)}{d\xi^*} = \frac{2\varphi_{13}^*}{\kappa^* \cos\varphi \sin\theta} - \frac{4\kappa^* \cos\varphi \sin\theta \varphi_{13}^*}{\kappa^{*2} \sin^2\theta + \xi^{*2}} + \frac{2a^*Ri\xi^*\gamma_1^*}{\kappa^{*2} \sin^2\theta + \xi^{*2}}$$

$$+ 2 \frac{\kappa^{*2} \sin^2\theta + \xi^{*2}}{a^*\kappa^* \cos\varphi \sin\theta} \varphi_{11}^* \tag{64}$$

$$\frac{d\varphi_{11}^*(\xi^*)}{d\xi^*} = \frac{2\varphi_{13}^*}{\kappa^* \cos\varphi \sin\theta} - \frac{2a^*Ri\gamma_3^*}{\kappa^* \cos\varphi \sin\theta} + 2 \frac{\kappa^{*2} \sin^2\theta + \xi^{*2}}{a^*\kappa^* \cos\varphi \sin\theta} \varphi_{ii}^* \tag{65}$$

$$\frac{d\gamma_1^*(\xi^*)}{d\xi^*} = \frac{\varphi_{13}^*}{a^*\kappa^* \cos\varphi \sin\theta} + \frac{a^*Ri\xi^*\delta^*}{\kappa^{*2} \sin^2\theta + \xi^{*2}} - \left(\frac{2\kappa^* \cos\varphi \sin\theta}{\kappa^{*2} \sin^2\theta + \xi^{*2}} - \frac{1}{\kappa^* \cos\varphi \sin\theta}\right)\gamma_3^*$$

$$+ \left(\frac{1}{Pr} + 1\right) \frac{\kappa^{*2} \sin^2\theta + \xi^{*2}}{a^*\kappa^* \cos\varphi \sin\theta} \gamma_1^* \tag{66}$$

For integrating these equations, ξ^* starts at

$$\xi_0^* = \kappa^* \cos\theta + a^*\kappa^* \cos\varphi \sin\theta$$

where

$$\varphi_{33}^{*}(\xi^{*}) = \left(\frac{1}{12\pi^{2}}\right)\kappa^{*2}\sin^{2}\theta$$

$$\varphi_{13}^{*}(\xi^{*}) = -\left(\frac{1}{12\pi^{2}}\right)\kappa^{*}\cos\varphi\,\sin\theta\,\xi_{0}^{*}$$

$$\varphi_{11}^{*}(\xi^{*}) = \frac{1}{12\pi^{2}}\left(\kappa^{*2}\sin^{2}\varphi\,\sin^{2}\theta + \xi_{0}^{*2}\right)$$

$$\varphi_{ii}^{*}(\xi^{*}) = \frac{1}{6\pi^{2}}\left(\kappa^{*2}\sin^{2}\theta + \xi_{0}^{*2}\right)$$

$$\gamma_{i}^{*}(\xi^{*}) = \delta^{*}(\xi^{*}) = 0$$

and goes to $\kappa^{*}\cos\theta$ where

$$\varphi_{ij}^{*}(\xi^{*}) = \varphi_{ij}^{*}(\kappa^{*}\cos\theta)$$

$$\gamma_{i}^{*}(\xi^{*}) = \gamma_{i}^{*}(\kappa^{*}\cos\theta)$$

$$\delta^{*}(\xi^{*}) = \delta^{*}(\kappa^{*}\cos\theta)$$

The integrations were carried out numerically on a high-speed computer for various fixed values of κ^{*}, θ, φ, a, and Ri. Directionally integrated spectrum functions can be obtained from (refs. 6 and 7)

$$\begin{bmatrix}\Psi_{ij}\\ \Gamma_{i}\\ \Delta\\ \Lambda_{ij}\\ \Psi'_{ij}\\ \Lambda'_{ij}\end{bmatrix} = \int_{0}^{\pi}\int_{0}^{2\pi}\begin{bmatrix}\varphi_{ij}\\ \gamma_{i}\\ \delta\\ \Omega_{ij}\\ \varphi'_{ij}\\ \Omega'_{ij}\end{bmatrix}\kappa^{2}\sin\theta\,d\varphi\,d\theta \qquad (67)$$

In this equation, Ω_{ij} is the vorticity spectrum tensor given by reference 8.

$$\Omega_{ij} = (\delta_{ij}\kappa^2 - \kappa_i\kappa_j)\varphi_{kk} - \kappa^2\varphi_{ij} \tag{68}$$

The primed quantities φ'_{ij} and Ω'_{ij} give, respectively, components of φ_{ij} and Ω_{ij} in a coordinate system rotated 45^o about the x_2-axis from the x_1-axis toward the x_3-axis. Since φ_{ij} and Ω_{ij} are second order tensors, components in the rotated system are (ref. 9)

$$\begin{bmatrix} \varphi'_{11} \\ \Omega'_{11} \end{bmatrix} = \frac{1}{2}\begin{bmatrix} \varphi_{11} \\ \Omega_{11} \end{bmatrix} + \begin{bmatrix} \varphi_{13} \\ \Omega_{13} \end{bmatrix} + \frac{1}{2}\begin{bmatrix} \varphi_{33} \\ \Omega_{33} \end{bmatrix} \tag{69}$$

and

$$\begin{bmatrix} \varphi'_{33} \\ \Omega'_{33} \end{bmatrix} = \frac{1}{2}\begin{bmatrix} \varphi_{11} \\ \Omega_{11} \end{bmatrix} - \begin{bmatrix} \varphi_{13} \\ \Omega_{13} \end{bmatrix} + \frac{1}{2}\begin{bmatrix} \varphi_{33} \\ \Omega_{33} \end{bmatrix} \tag{70}$$

The spectrum functions given by equation (67) can be integrated over all wave numbers to give

$$\begin{bmatrix} \overline{u_iu_j} \\ \overline{\tau u_i} \\ \overline{\tau^2} \\ \overline{\omega_i\omega_j} \\ \overline{u_iu_j}' \\ \overline{\omega_i\omega_j}' \end{bmatrix} = \int_0^\infty \begin{bmatrix} \Psi_{ij} \\ \Gamma_i \\ \Delta \\ \Lambda_{ij} \\ \Psi'_{ij} \\ \Lambda'_{ij} \end{bmatrix} d\kappa \tag{71}$$

where the primes again refer to components in a coordinate system rotated 45^o. Computed spectra and correlations will be considered in the next section.

RESULTS AND DISCUSSION

All the calculated results given in this section are for a gas with a Prandtl number of 0.7. Dimensionless energy spectra $\left(\text{spectra of } \overline{u_iu_i^*}\right)$ and spectra of $\overline{\tau^2}^*$ are plotted

in figures 1 and 2. The spectra are plotted for several values of $a^* = (t - t_0)dU_1/dx_3$ and of $g^* = \beta g(t - t_0)^2\, dT/dx_3$. The parameter g^* rather than the Richardson number $Ri = \beta g\, dT/dx_3 / (dU_1/dx_3)^2$ is used here since the use of g^* and a^* enables us to consider buoyancy and shear effects separately. (The Richardson number contains both buoyancy and shear effects.) The quantity g^* is related to Ri and a^* by the equation

$$g^* = a^{*2}Ri \tag{72}$$

When plotted by using the similarity variables shown in figures 1 and 2, the dimensionless spectra for no buoyancy and shear effects $g^* = a^* = 0$ do not change with time, and thus comparison of the various curves indicates how buoyancy and shear effects will alter the spectra. Thus, if a dimensionless-spectrum curve lies above the curve for $g^* = a^* = 0$, the turbulent activity for that case is greater than it would be for no buoyancy and shear effects. The turbulence itself decays with time, as in references 1 and 2.

Positive values of the buoyancy parameter g^* correspond to stabilizing conditions, and negative values correspond to destabilizing conditions. Figures 1 and 2 show that the trends with g^* for a case with shear ($a^* = 2$) are similar to those from reference 1 for no shear ($a^* = 0$). That is, in the destabilizing case, buoyancy forces tend to feed energy

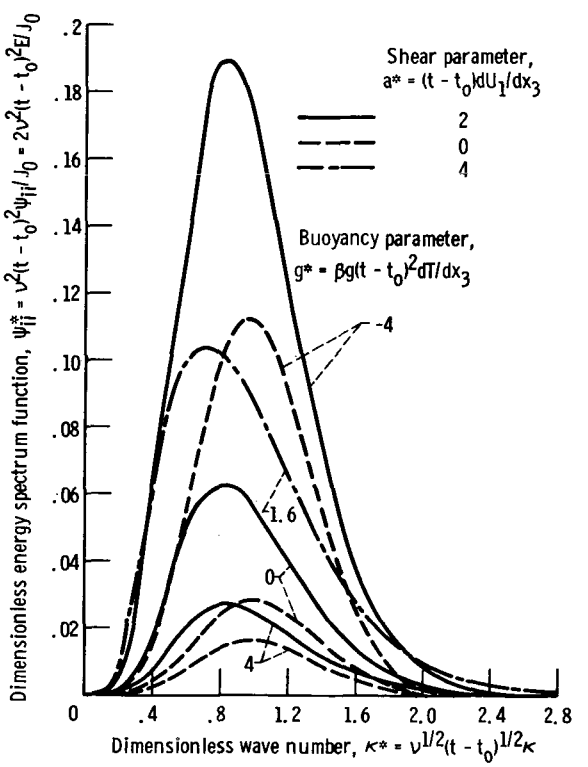

Figure 1. - Dimensionless spectra of turbulent energy $\overline{u_i u_i}^*$. Prandtl number, 0.7.

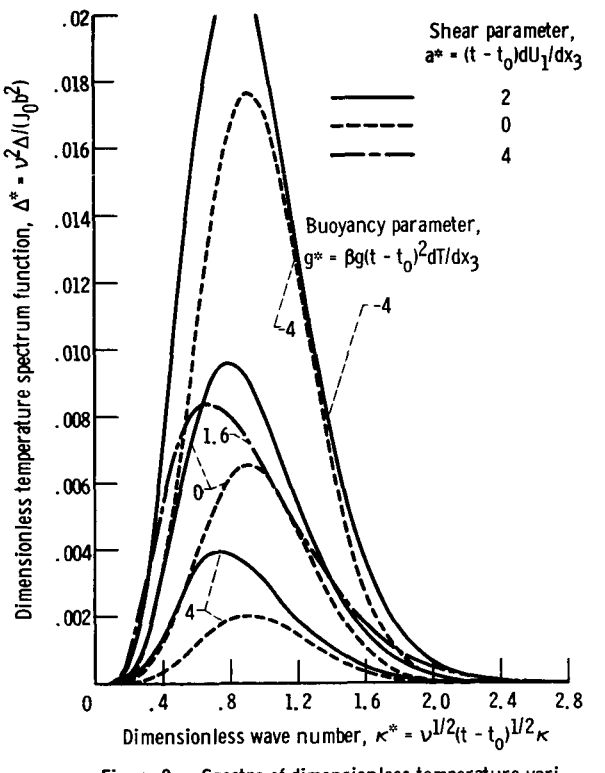

Figure 2. - Spectra of dimensionless temperature variance $\overline{\tau^2}^*$. Prandtl number, 0.7.

or activity into the turbulent field, whereas in the stabilizing case they tend to extract it. Comparison of the curves with shear (solid curves) with those without shear (dashed curves) for values of g* of -4, 0, and 4 indicates that for all three cases the effect of the shear is to feed energy or activity into the turbulent field. Thus for the destabilizing case, the buoyancy and shear have similar effects; but for the stabilizing case, they have opposite effects. Comparison of the curve in figure 1 for $g^* = 4$ and $a^* = 2$ with that for $a^* = g^* = 0$ indicates that for the former curve the energy added by the shear effects approximately balances that extracted by buoyancy but that the wave number distributions for the two processes are slightly different.

As a* increases, the spectra become asymmetric, the slopes on the high-wave-number sides of the curves becoming more gradual. The dot-dashed curves for an a* of 4 and a g* of 1.6 are plotted to show this effect. As in references 2, 6, and 7, the effect is due to the transfer of energy or activity into the high-wave-number regions by the transfer term associated with the mean velocity gradient (see the discussion in the paragraph following eq. (38)).

The buoyancy forces might be expected to act more strongly on the turbulent velocity components lying in the direction of those forces than on the other components. This expectation is confirmed in the plot of $\overline{u_3^2}/\overline{u_1^2}$ for $a^* = 0$ in figure 3. The ratio $\overline{u_3^2}/\overline{u_1^2}$ is greater than 1 in the destabilizing case and less than 1 in the stabilizing case. However, although $\overline{u_3^2}/\overline{u_1^2}$ becomes small, it does not approach zero for highly stable conditions. Apparently $\overline{u_1^2}$ begins to decrease as rapidly as, or more rapidly than $\overline{u_3^2}$, as g* becomes large.

The voriticity component ratio $\overline{\omega_3^2}/\overline{\omega_1^2}$ is also plotted in figure 3. The trends for $\overline{\omega_3^2}/\overline{\omega_1^2}$ are opposite to those for $\overline{u_3^2}/\overline{u_1^2}$. For the stabilizing case, the voriticity tends to be alined in the direction of the buoyancy forces. The turbulent velocities associated with that vorticity will then tend to be normal to the buoyancy forces, in agreement with the curve for $\overline{u_3^2}/\overline{u_1^2}$. For the destabilizing case, the vorticity tends to lie in directions normal to the buoyancy forces. That will tend to increase $\overline{u_3^2}/\overline{u_1^2}$ as shown in figure 3, although the ratio will not approach infinity, because even if all the vorticity lies in directions normal to the buoyancy forces, $\overline{u_1^2}$ or $\overline{u_2^2}$ will not be zero.

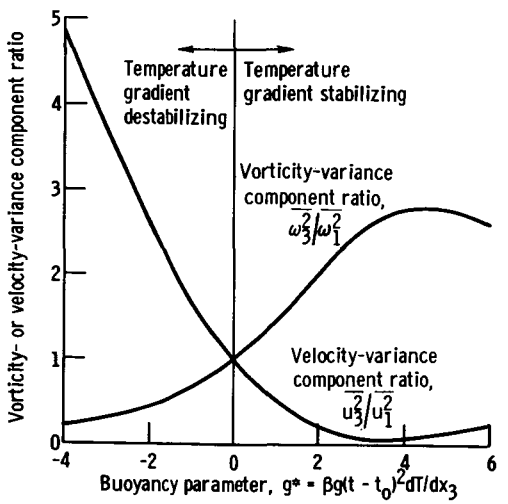

Figure 3. - Velocity and vorticity-variance component ratios plotted against buoyancy parameter for case of no shear. Prandtl number, 0.7.

In the preceding discussion, the effect of buoyancy forces were considered on the turbu-

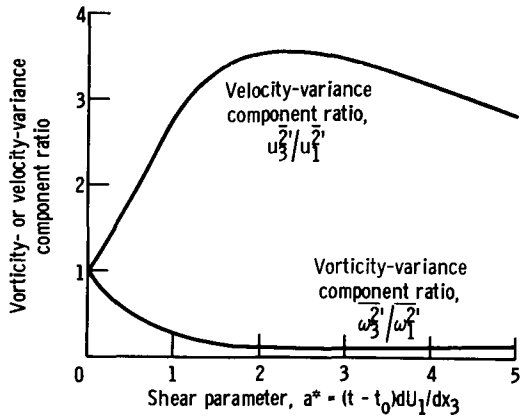

Figure 4. - Velocity- and vorticity-variance component ratios in coordinate system rotated 45° plotted against shear parameter for case of no buoyancy effects.

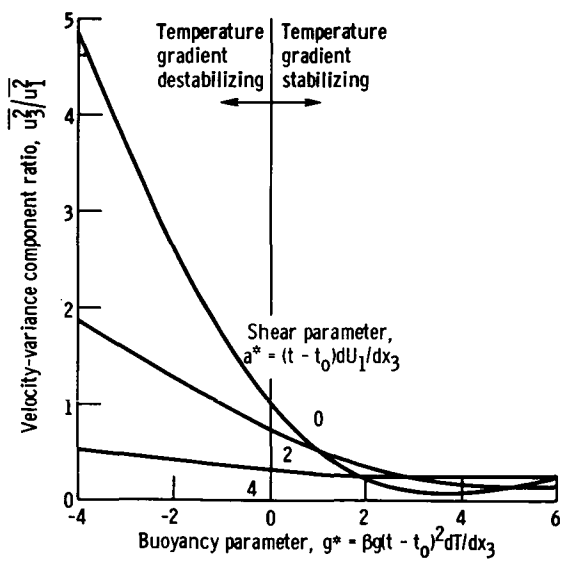

Figure 5. - Plot showing velocity-variance component ratio $\overline{u_3^2}/\overline{u_1^2}$ as a function of buoyancy and shear parameters. Prandtl number, 0.7.

lence components without mean shear. Next, consider the case of shear with no buoyancy effects. In that case, the turbulent vorticity (or vortex filaments) would be expected to tend to aline in the direction of maximum strain, which is at 45° to the mean velocity. Figure 4 shows turbulent vorticity and velocity components ratios in a coordinate system rotated 45° counterclockwise about the x_2-axis. If the vorticity were all alined in the direction of maximum strain, $\overline{\omega_3^{2'}}/\overline{\omega_1^{2'}}$ would be zero. The curve shows that there is a strong tendency for that alinement to occur at moderate values of a*, but the degree of alinement does not continue to improve as a* becomes large. The tendency for the vortex filaments to aline in the direction of maximum strain is reflected in the trend for the turbulent velocity components to become maximum in a direction normal to the maximum strain, as shown in the curve for $\overline{u_3^{2'}}/\overline{u_1^{2'}}$. The degree of alinement, however, does not continue to improve as a* becomes large.

Combined effects of buoyancy and shear on $\overline{u_3^2}/\overline{u_1^2}$ are shown in figure 5. The curves show that for no buoyancy effects (g* = 0) the turbulence component $\overline{u_3^2}$, which is in the direction of the mean velocity gradient, is reduced in comparison with $\overline{u_1^2}$ by the shear. This trend also occurs for negative (destabilizing) values of g* and for small positive (stabilizing) values of g*. For more strongly stabilizing conditions, the trends become more complex, and the curves cross over one another.

The effects of buoyancy and shear are considered separately in figure 5, which utilizes the parameters g* and a*. Since the Richardson number contains both buoyancy and shear effects, one might suppose that its use would reduce or eliminate the need for another parameter. Figure 6 shows that is not the case, since $\overline{u_3^2}/\overline{u_1^2}$ is a strong function of both Richardson number and a*.

The ratio of two turbulence components which are normal to the body forces and

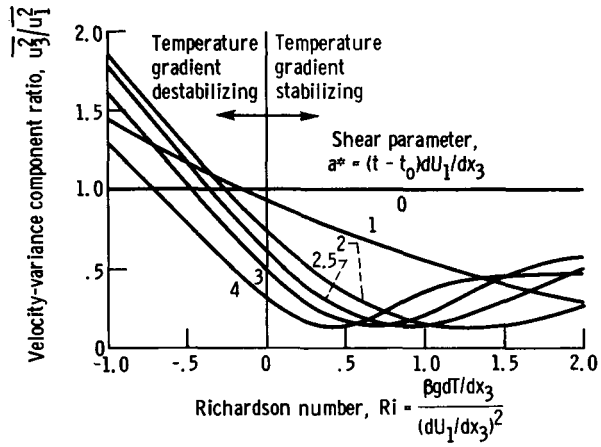

Figure 6. - Plot showing velocity-variance component ratio $\overline{u_3^2}/\overline{u_1^2}$ as a function of Richardson number and shear parameter. Prandtl number, 0.7.

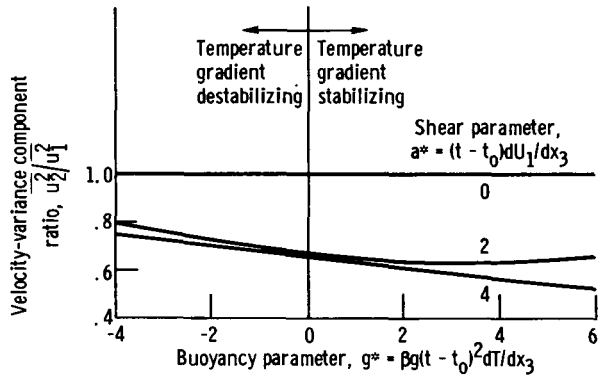

Figure 7. - Plot showing velocity-variance component ratio $\overline{u_2^2}/\overline{u_1^2}$ as a function of buoyancy and shear parameters.

mean velocity gradient plotted as a function of g* and a* are shown in figure 7. For no shear (a* = 0), $\overline{u_2^2}/\overline{u_1^2}$ is 1 since the turbulence is axially symmetric. For $a^* \neq 0$, the shear tends to destroy the axial symmetry and to reduce $\overline{u_2^2}/\overline{u_1^2}$ below 1.

Consider next the turbulent heat transfer and the turbulent shear stress. Temperature-velocity correlation coefficients $-\overline{\tau u_3}\Big/\left(\overline{\tau^2}\right)^{1/2}\left(\overline{u_3^2}\right)^{1/2}$ are plotted in figure 8. The correlation $\overline{\tau u_3}$ is proportional to the turbulent heat transfer in the direction of the temperature gradient. The unusual feature of these results is that $\overline{\tau u_3}$ changes sign as g* becomes large. That is, for very stable conditions, the turbulence begins to pump heat against the temperature gradient. This phenomenon was observed in the results of reference 1 for an a* of zero. As a* increases, the value of g* at which $\overline{\tau u_3}$ changes sign increases.

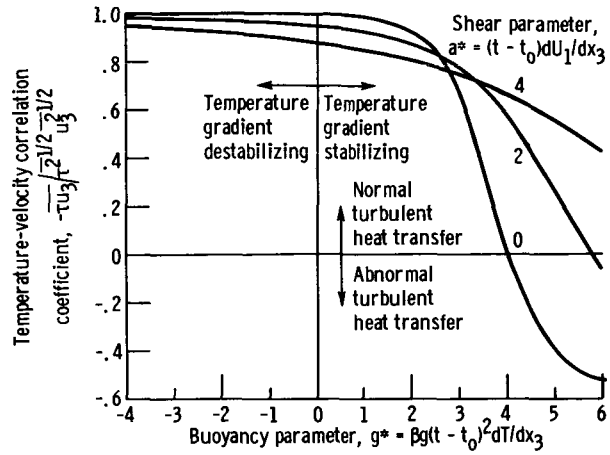

Figure 8. - Plot showing temperature-velocity correlation coefficient $-\overline{\tau u_3}/\overline{\tau^2}^{1/2}\overline{u_3^2}^{1/2}$ as a function of buoyancy and shear parameters. Prandtl number, 0.7.

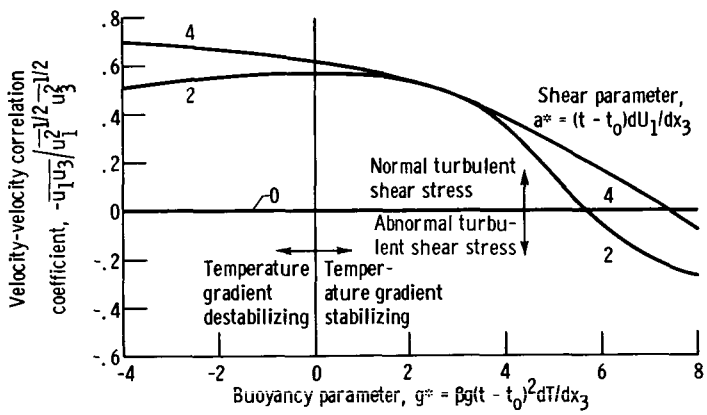

Figure 9. - Plot showing velocity-velocity correlation coefficient $-\overline{u_1 u_3}/\overline{u_1^2}^{1/2}\overline{u_3^2}^{1/2}$ as a function of buoyancy and shear parameters.

Velocity-velocity correlation coefficients for shear are plotted in figure 9. At small values of g*, the trends with a* are opposite to those for figure 8; the values of $\overline{u_1 u_3}\Big/\left(\overline{u_1^2}\right)^{1/2}\left(\overline{u_3^2}\right)^{1/2}$ are zero for $a^* = 0$, while the value of $-\overline{\tau u_3}\Big/\left(\overline{\tau^2}\right)^{1/2}\left(\overline{u_3^2}\right)^{1/2}$ are close to 1 for small a* and g*. As was the case for $\overline{\tau u_3}$, $\overline{u_1 u_3}$ changes sign as g* becomes large. As conditions become strongly stabilizing, the turbulence begins to pump the fluid in such a way as to tend to increase the velocity gradient. Thus, there occurs, for sufficiently large values of g*, a negative eddy viscosity as well as a negative eddy conductivity. Although a negative eddy conductivity can occur with only buoyancy effects present, the occurrence of a negative eddy viscosity requires combined buoyancy and shear effects.

A possible explanation for the theoretically observed negative eddy viscosity and conductivity can be given in terms of a modified mixing length theory as illustrated in

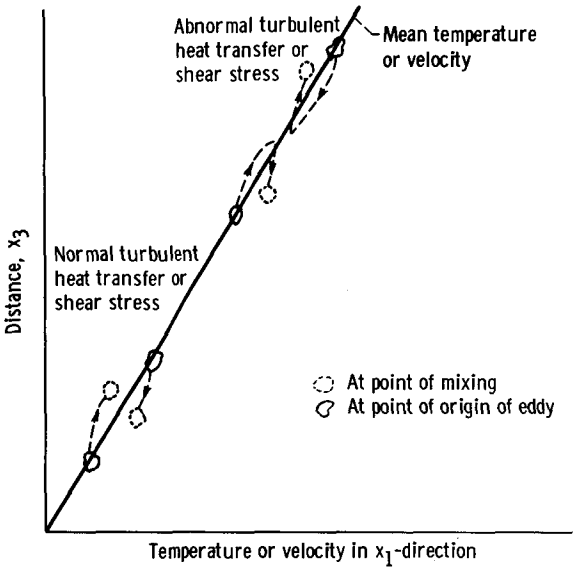

Figure 10. - Sketch illustrating possible mechanism for producing negative eddy conductivity and viscosity.

figure 10. Normal turbulent heat transfer or shear stress is shown in the left portion of the figure. An eddy originating at the mean velocity and temperature of the fluid at a point may move either upward or downward. By conduction and viscous effects, it will tend to acquire the local mean temperature and velocity of the fluid as it moves, and thus its path will curve toward the mean velocity or temperature line. When the eddy mixes with the fluid, it will tend to decrease the mean temperature and velocity gradients. The effective eddy conductivity and viscosity will be positive since they act in the same direction as the molecular conductivity and viscosity.

By contrast, for the abnormal case where the buoyancy forces are strongly stabilizing, the original direction of motion of an eddy may be reversed. This reversal might happen because the buoyancy force, in the stabilizing case, acts in the direction opposite to that in which the eddy starts to move. Possible paths for the eddy on the distance-temperature or distance-velocity plane under these conditions are sketched on the right side of figure 10. As shown, the eddy path can cross the mean temperature or velocity line. As the eddy mixes with the fluid, it will then tend to increase the mean temperature and velocity gradients, and thus the effective eddy conductivity and viscosity will be negative. The actual mechanism may be more complicated than that considered here. The preceding explanation is given only to show that negative eddy conductivities and viscosities are physically reasonable. The turbulent heat transfer and shear stress do not necessarily change sign at the same value of g^*, since the eddy paths on the distance-temperature plane and on the distance-velocity plane may be different because of differences between the conduction and viscous effects on the eddy as it moves. Comparison of figures 8 and 9 shows that the turbulent shear stress changes sign first as g^* increases.

The ratio of eddy conductivity to eddy viscosity plotted against g^* is shown in figure 11. The eddy conductivity and eddy viscosity are defined by the relations

$$\epsilon_h = -\frac{\overline{\tau u_3}}{\frac{dT}{dx_3}}$$

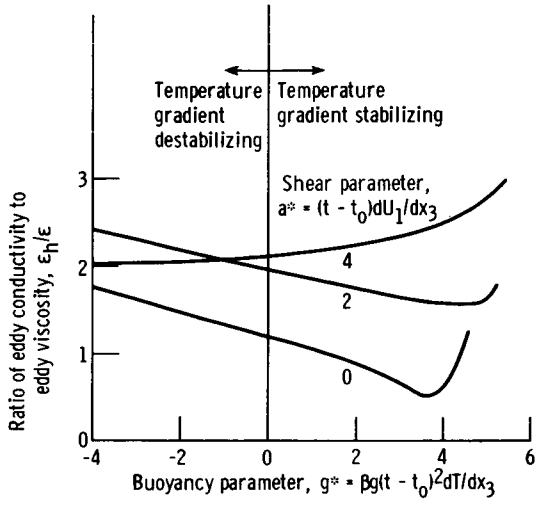

Figure 11. - Plot showing ratio of eddy conductivity to eddy viscosity as a function of buoyancy and shear parameters. Prandtl number, 0.7.

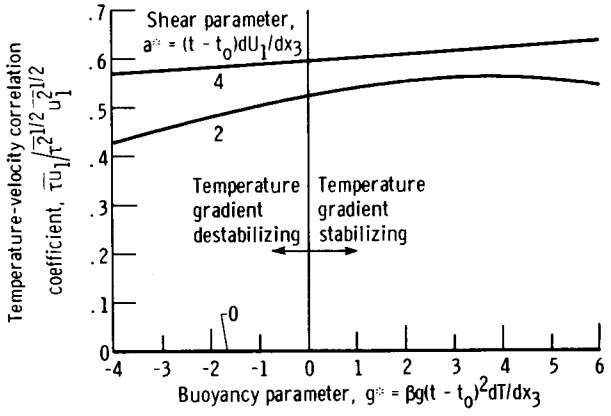

Figure 12. - Plot showing correlation coefficient $\overline{\tau u_1}/\overline{\tau^2}^{1/2}\overline{u_1^2}^{1/2}$ as a function of buoyancy and shear parameters. Prandtl number, 0.7.

and

$$\epsilon = -\frac{\overline{u_1 u_3}}{\dfrac{dU_1}{dx_3}}$$

The ratio ϵ_h/ϵ is calculated from $\overline{\tau u_3^*}\Big/\left(\overline{u_1 u_3^*}/a^*\right)$. For small values of a*, ϵ_h/ϵ decreases with increasing g* except for large g*. For an a* of 4, ϵ_h/ϵ increases with increasing g*. The sharp increases in ϵ_h/ϵ near the ends of the curves occur because the eddy viscosity approaches zero and changes sign near those points.

Values of the correlation coefficient $\overline{\tau u_1}\Big/\left(\overline{\tau^2}\right)^{1/2}\left(\overline{u_1^2}\right)^{1/2}$ are presented in figure 12. The correlation $\overline{\tau u_1}$ is proportional to turbulent heat transfer in the x_1-direction. The fact that there should be heat transfer in the x_1-direction is surprising since there is a temperature gradient only in the x_3-direction. It appears, however, that $\overline{\tau u_1}$ can be nonzero because of the nonzero values of $\overline{\tau u_3}$ and $\overline{u_1 u_3}$. Since there is a correlation between τ and u_3 and between u_3 and u_1, the fact that a correlation should occur between τ and u_1 seems reasonable. It must be admitted, though, that heat transfer in a direction of zero temperature gradient runs contrary to normal intuition. It should be noted that the effect is not dependent on the presence of buoyancy forces (i. e., g* can be zero). The turbulent heat transfer in the x_1-direction is not necessarily small compared with that in the x_3-direction. Figure 13, which shows plotted values of $-\overline{\tau u_3}\Big/\overline{\tau u_1}$, indicates that the turbulent heat transfer in the two directions can be of the same order of magnitude.

Comparison of the present analytical results with available experimental data is of

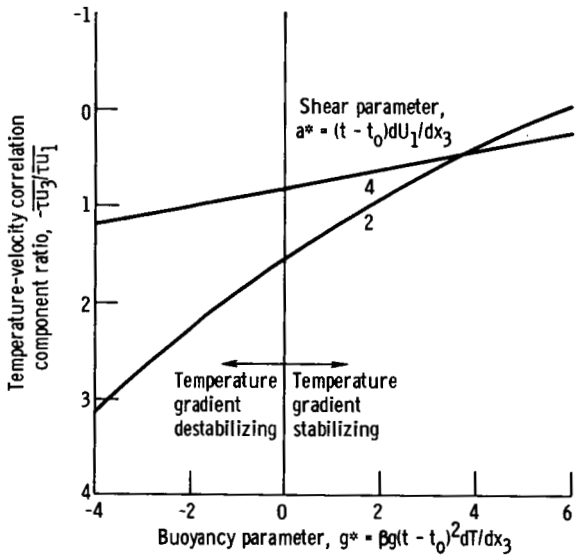

Figure 13. - Plot showing temperature-velocity correlation component ratio $-\overline{\tau u_3}/\overline{\tau u_1}$ as a function of buoyancy and shear parameters.

interest in order to see if there is a correspondence. Experimental data for grid-generated turbulence in the presence of combined buoyancy and shear effects are presented in references 10 and 11. A comparison between analysis and the data obtained at station 5 in reference 11 is given in figure 14. The various turbulence ratios are plotted against Richardson number rather than against g^*, since $(t - t_o)$ in g^* is hard to estimate because of uncertainties in the initial and other conditions in the experiment. For the same reason, no attempt is made to calculate $a^* = (t - t_o)\, dU_1/dx_3$ directly for the experiment. The data and analysis for $\overline{u_3^2}/\overline{u_1^2}$ at Ri = 0 indicate a value for a^* of about 2, and that value is used throughout the comparison. A reasonable correspondence

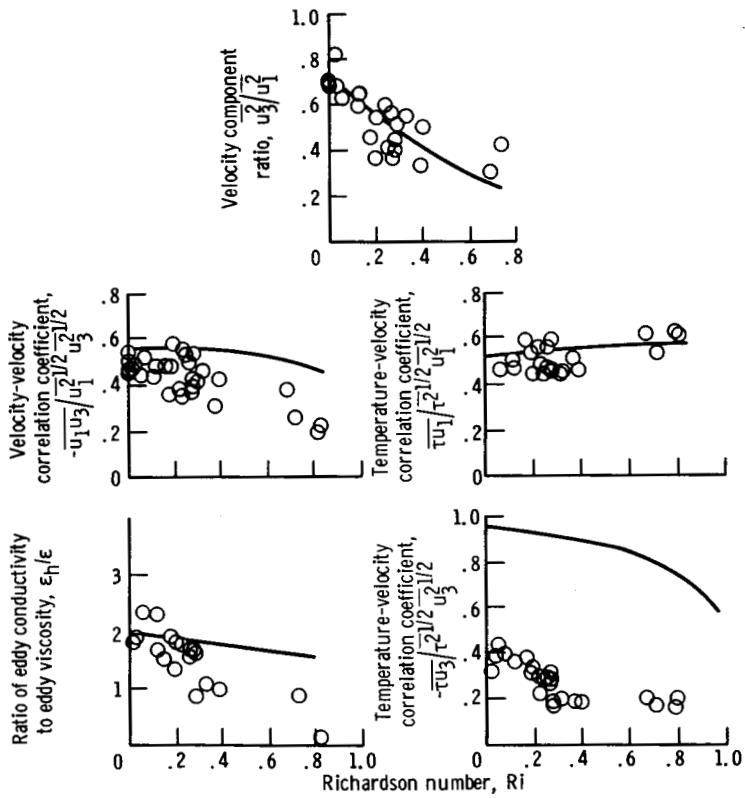

Figure 14. - Comparison of analytical results with experimental data at station 5 in reference 11. Shear parameter, $a^* = 2$.

exists between analysis and experiment for the various turbulence ratios and correlation coefficients except in the last plot. Conditions in the analysis and experiment differ. For instance, the analysis assumes that the temperature fluctuations arise from the interaction of the mean temperature gradient with the turbulence whereas in the experiment the heated grid probably produced temperature fluctuations. A disconcerting aspect of the experimental data is that it shows an increase in turbulence level with distance while the analysis shows a decrease. The increase shown in the experiment might be caused by lateral inhomogenieties in the turbulence, boundary layer effects, or by triple correlation effects. All these effects were neglected in the analysis.

SUMMARY OF RESULTS

The analytical results for combined effects of vertical buoyancy forces and vertical velocity gradients indicate that, as in the case of no shear, destabilizing buoyancy forces can feed energy or activity into a turbulent field whereas stabilizing buoyancy forces can extract it. The effect of the shear is to feed energy or activity into the turbulent field. Thus for the destabilizing case, the buoyancy and shear have similar effects; but for the stabilizing case, they work in opposite directions.

Energy or activity transfer between wave numbers by the stretching of turbulent vortex filaments by the mean velocity gradient causes the spectra to become asymmetric; the slopes on the high-wave-number sides of the spectra become more gradual.

For the destabilizing case, buoyancy forces tend to increase the vertical turbulence component in comparison to the horizontal component in the flow direction while the shear tends to decrease it. For weakly stabilizing conditions both the buoyancy and shear tend to decrease the ratio of vertical to horizontal turbulence components. For more strongly stabilizing conditions, the trends become less well defined.

The shear tends to aline the turbulent vorticity in the direction of maximum mean strain, which is 45° from the flow direction. Destabilizing buoyancy forces tend to aline the vorticity in horizontal directions whereas stabilizing forces tend to aline it vertically.

When buoyancy forces are strongly stabilizing, the eddy conductivity and viscosity can be negative. This result appears reasonable when considered from the standpoint of a modified mixing length theory. Turbulent heat transfer occurs in a horizontal as well as a vertical direction, even though the velocity and temperature gradients are both vertical.

Comparison of analytical with experimental results indicates that the former bear a

reasonable correspondence with results for observed turbulence, although the conditions in the experiment differed somewhat from those assumed in the analysis.

Lewis Research Center,
National Aeronautics and Space Administration,
Cleveland, Ohio, November 22, 1966,
129-01-09-07-22.

APPENDIX - SYMBOLS

a	vertical velocity gradient, dU_1/dx_3
a^*	shear parameter, defined by eq. (56)
b	vertical temperature gradient, dT/dx_3
g	$-g_3$, vertical body force/unit mass in $-x_3$-direction (gravitational force/unit mass)
g_3	vertical body force/unit mass
g_i	body force component/unit mass
g^*	buoyancy parameter, $\beta g(t - t_0)^2 \, dT/dx_3$
J_0	constant that depends on initial conditions
Pr	Prandtl number, ν/α
p	pressure
$\vec{r}, r_i$	vector between points P and P'
Ri	Richardson number, defined by eq. (57)
T	mean temperature
t	time
U_i	mean velocity component
u_i	fluctuating velocity component
$\overline{u_i u_j}^*$	$\dfrac{\nu^{5/2}(t - t_0)^{5/2}}{J_0} \overline{u_i u_j}$
x_i	space coordinate
α	thermal diffusivity
β	expansion coefficient
Γ_j	defined by eq. (67)
γ_i	defined by eq. (21)
γ_i'	defined by eq. (22)
γ_i^*	defined by eq. (54)
Δ	defined by eq. (67)
δ	defined by eq. (23)
δ_{ij}	Kronecker delta
δ^*	defined by eq. (55)
ϵ	eddy viscosity
ϵ_h	eddy conductivity
ζ	defined by eq. (19)
ζ'	defined by eq. (20)
η	running or dummy variable that equals t when $\xi = \kappa_3$
θ, φ	angular coordinates (see eq. (59))
κ_i	wave number component
κ_i^*	defined by eq. (51)
Λ_{ij}	defined by eq. (67)
λ_i	defined by eq. (17)
λ_i'	defined by eq. (18)
ν	kinematic viscosity
ξ	running or dummy variable for which κ_3 is a particular value
ρ	density
τ	temperature fluctuation
$\overline{\tau u_i}$	temperature-velocity correlation
$\overline{\tau u_i}^*$	$\dfrac{\nu^{5/2}(t - t_0)^{3/2}}{J_0} \dfrac{\overline{\tau u_i}}{b}$

$\overline{\tau^{2*}}$ $\quad \dfrac{\nu^{5/2}(t - t_0)^{1/2}}{J_0 b^2}\overline{\tau^2}$

φ_{ij} defined by eq. (16)

φ^*_{ij} defined by eq. (53)

Ψ_{ij} defined by eq. (67)

Ψ^*_{ij} $\quad \Psi_{ij}\dfrac{\nu^2(t - t_0)^2}{J_0}$

Ω_{ij} given by eq. (68)

$\overline{\omega_i\omega_j}$ turbulent vorticity variance

Subscripts:

0 at virtual origin of turbulence where turbulent energy would be infinite (It is assumed that turbulence is isotropic at x_0 and that velocity and temperature gradients begin to act there)

1 in flow direction

3 in vertical direction, which is direction of mean velocity gradient and buoyancy force

Superscripts:

' at point P', also refers to coordinate system rotated 45^o

* on dimensionless quantities

– over averaged quantities

REFERENCES

1. Deissler, Robert G.: Turbulence in the Presence of a Vertical Body Force and Temperature Gradient. J. Geophys. Res., vol. 67, no. 8, July 1962, pp. 3049-3062.
2. Deissler, Robert G.: Effects of Inhomogeneity and of Shear Flow in Weak Turbulent Fields. Phys. Fluids, vol. 4, no. 10, Oct. 1961, pp. 1187-1198.
3. Ellison, T. H.: Turbulent Transport of Heat and Momentum from an Infinite Rough Plane. J. Fluid Mech., vol. 2, pt. 5, July 1957, pp. 456-466.
4. Townsend, A. A.: Turbulent Flow in a Stably Stratified Atmosphere. J. Fluid Mech., vol. 3, p. 4, Jan. 1958, pp. 361-372.
5. Landau, L. D.; and Lifshitz, E. M. (J. B. Sykes and W. H. Reid, trans.): Fluid Mechanics. Addison-Wesley Publishing Co., 1959, p. 212.
6. Deissler, Robert G.: Turbulent Heat Transfer and Temperature Fluctuations in a Field With Uniform Velocity and Temperature Gradients. Int. J. Heat Mass Transfer, vol. 6, Apr. 1963, pp. 257-270.
7. Deissler, Robert G.: Weak Locally Homogeneous Turbulence in Idealized Flow through a Cone. NASA TN D-3613, 1966.
8. Batchelor, George K.: The Theory of Homogeneous Turbulence. Cambridge University Press, 1953, p. 39.
9. Hinze, J. O.: Turbulence; an Introduction to its Mechanism and Theory. McGraw-Hill Book Co., Inc., 1959, p. 570.
10. Ellison, T. H.: Laboratory Measurements of Turbulent Diffusion in Stratified Flows. J. Geophys. Res., vol. 67, no. 8, July 1962, pp. 3029-3031.
11. Webster, C. A. G.: An Experimental Study of Turbulence in a Density-Stratified Shear Flow. J. Fluid Mech., vol. 19, p. 2, June 1964, pp. 221-245.